Boreal Forest Wildfire and Climate Linked Drivers of Carbon and Nitrogen Loss

Johan Eckdahl[1,2], Jeppe Kristensen[3], and Daniel Metcalfe[2]

[1]Department of Physical Geography and Ecosystem Science, Lund University, Lund, Sweden
[2]Department of Ecology and Environmental Science, Umeå University, Umeå, Sweden
[3]School of Geography and the Environment, University of Oxford, Oxford, United Kingdom

Correspondence: Johan Eckdahl (Johan.Eckdahl@nateko.lu.se)

Abstract. The boreal landscape covers large portions of the earth's land area and stores a significant percentage of its terrestrial carbon (C). Increased emissions due to climate change amplified fire frequency, size and intensity threaten to remove elements such as C and nitrogen (N) from forest soil and vegetation at rates faster than they accumulate. This may result in large areas within the region becoming a net source of greenhouse gases creating a positive feedback loop with a changing climate.

5   Estimates of per area fire emissions are regionally limited and knowledge of their relation to climate and ecosystem properties is sparse. This study sampled 50 separate Swedish wildfires from 2018 providing quantitative estimates of C and N loss due to fire along a climate gradient. Mean annual precipitation had strong positive effects on total fuel, which was the strongest driver for increasing C and N losses, while mean annual temperature (MAT) had greater influence on both pre- and postfire fuel bulk and chemical properties which had mixed effects on C and N losses. Significant fire induced loss of C occurred in the 50

10 plots comparable to estimates in similar Eurasian forests but approximately a quarter of those found in typical North American boreal wildfires. N loss was insignificant though large proportions were collected from lower soil layers to a surface layer of char in proportion to increased MAT. These results reveal the variability of C and N losses between global regions and across local climate conditions and a need to better incorporate these factors into models to improve estimates of global emissions of C and N due to fire in future climate scenarios. Additionally, this study demonstrated the linkage between climate and the

15 chemical transformation of residual soil fuel and discusses its potential for altering C and N dynamics in postfire recovery.

1 Introduction

Worldwide, boreal forests account for a net C sink into plants and soil of 0.31 ± 0.19 Pg of C per year, equivalent to $27.3 \pm 16.7\%$ of the planet's terrestrial C sink (Tagesson et al., 2020). This sink plays a pivotal role in the greenhouse gas

20 content of the atmosphere (Lemprière et al., 2013). Low temperatures and waterlogged soil conditions slow decomposition of centuries of litter additions resulting in the build up of thick layers of soil organic material where the majority of C is stored (Malhi et al., 1999; Rapalee et al., 1998). The balance of C transfer between atmospheric and terrestrial stocks on the

yearly timescale is dictated by rates of terrestrial net primary production and respiration which are strongly controlled by temperature, moisture and nitrogen (N) availability (Deluca and Boisvenue, 2012).

25 The predominant disturbance to this C balance is approximately centurial outbreaks of wildfire (Bond-Lamberty et al., 2007). Among the immediate effects of fire are a substantial release of C to the atmosphere from soil and vegetation (Schultz et al., 2008) as well as physical restructuring of the habitat through varying degrees of over- and understory removal and changes in soil properties such as bulk density (Certini, 2005). Further, bioavailability of energy sources and nutrients is substantially affected as elements such as C and N are lost and chemical structure altered by heating, i.e. charred (Neff et al., 2005). Along

30 with a changing climate, these effects have the power to influence community structure and process rates shaping future forest C and N cycles on decadal to centurial timescales (Johnstone et al., 2020; Mekonnen et al., 2019). Changing patterns of temperature and precipitation in recent decades have caused increases in frequency, intensity and size of fires with further amplification predicted in the future (de Groot et al., 2013b; Gillett et al., 2004; Kelly et al., 2013; de Groot et al., 2003). Escalating additions of C to the atmosphere due to fire and changing C cycling in recovering ecosystems may accelerate

35 climate change (Li et al., 2017).

Both long and short term processes have been identified as drivers of the dynamics of fire events. Particularly, the strongest driver of per area emissions of C in boreal wildfires appears to be total fuel (i.e. potentially combustible organic material) which is strongly controlled by long term forest moisture (Walker et al., 2018, 2020). However, in order for this fuel to be available to ignite and propagate fire it must be sufficiently dried and spatially arranged to be susceptible to high heat and

40 oxygen exposure during active fire. These factors dictate fuel availability, a highly temporal measure of the proportion of total fuel that is readily combustible. Therefore boreal wildfire models often incorporate short term fire weather variables (e.g. drought indices, temperature, wind speed, relative humidity) as well as separate fuel loads into compartments such as surface litter, which influences ignition and rate of spread, and the more compactly arranged layers below, which act as a heat reservoir that supports extending smoldering over days to weeks (de Groot et al., 2003; Van Wagner, 1987; Rabin et al., 2017; Kasischke

45 et al., 2005; Wiggins et al., 2020). Spatial arrangement of overstory fuel loads has also been shown to have a strong impact on fire severity and intensity and distinguishes the boreal wildfire regimes of the North American and Eurasian continents (Rogers et al., 2015). Furthermore, climate has been observed to have a conditioning effect on fuel chemistry through its control over the type of detrital inputs and their decomposition state, which are often represented by the C:N weight ratio in soils (Vanhala et al., 2008; Kohl et al., 2018). Fuel chemistry, arrangement, moisture content, applied heat and oxygen availability in turn

50 have all been related to the efficiency of the combustion reaction during fire and therefore emission chemistry and the charring of remaining non-volatilized fuel (Schmidt and Noack, 2000). Production of charred material is an innately fire driven process and a representative measure of these interrelated effects. Because additions of char to soils have been observed to have strong impacts on C storage and nutrient cycling (Schmidt and Noack, 2000; Preston and Schmidt, 2006), fire induced transformation of remaining fuel is valuable to study alongside its loss from the ecosystem during wildfire.

55 Boreal C emissions due to wildfire are calculated by multiplying total area burned by estimates of emissions per area (French et al., 2004). While total area burned may be evaluated through remote sensing (Ruiz et al., 2012), per area emissions are generally derived from labor intensive field sampling which are extrapolated to the larger scale either directly or through weighting

by poorly constrained free parameters such as total fuel load (French et al., 2004; Soja et al., 2004). This field sampling has been regionally limited and biased towards a few high intensity burn complexes in North America which may in turn bias global

60 emission estimates (van Leeuwen et al., 2014). For example, the Eurasian boreal region is dominated by relatively fire resistant vegetation that promotes lower intensity fire (Rogers et al., 2015; de Groot et al., 2013a) and C loss (0.88 kgC/m^2) (Ivanova et al., 2011) than that in typical (Walker et al., 2020) North American wildfire (3.3 kgC/m^2) (Boby et al., 2010). Though Eurasia contains over 70% of the boreal global land area (de Groot et al., 2013a), and about 50% (20 Mha/yr) of its yearly burnt area (Rogers et al., 2015), wildfire emissions from this region are severely under sampled in the field (van Leeuwen

65 et al., 2014). Additionally, estimates of N loss from boreal wildfire are rare in all regions despite its well recognized role as a limiting nutrient and evidence of its immediate removal in percentages similar to C (Boby et al., 2010). Lastly, boreal wildfire research has often focused on individual or small groups of fires located relatively near to each other, with little information about the representativeness of the observations or context of the results within the broader spectrum of fire impacts across the wider region, especially those relating to variation in climate. This knowledge gap has thus far been addressed with con-

70 glomerated studies spanning different fire seasons, ecosystem types and research methodologies (Walker et al., 2020; Gaboriau et al., 2020). Therefore, widely replicated, simultaneous and systematic field measurements of fire processes in under sampled regions with particular attention to climate are needed to derive more robust, generalizable conclusions about boreal forest responses to wildfire.

This study sampled 50 separate fire complexes spanning broad gradients of mean annual temperature (MAT) and precipi-

75 tation (MAP) which ignited in Sweden during summer 2018 (Fig. 1). Analysis intended to distinguish the effects of climate on fire induced changes in C and N stocks with direct, fine scale measurements and little loss of generality thereby providing insight into both local processes and valuable, globally comparable data from an under sampled region. Space-for-time substitution (De Frenne et al., 2013) along with a control-impact design provided insight into the possible future conditions of Fennoscandian forests in a changing climate and fire regime. Specifically, it was hypothesized that:

80   1. Fire significantly reduced and spatially rearranged both C and N stocks.

    2. Loss of C and N stocks and their transfer to charred material were related to prefire total fuel amount, composition and arrangement amongst forest compartments.

    3. A direct relation between climate variables and fire induced C and N stock changes exists and is mediated by long term ecosystem properties as well as time-of-fire processes which are represented by the extent of charring of residual fuel.

85 ## 2 Materials and methods

2.1 Experimental design and field site selection

50 burnt plots were selected from a pool of 325 fires identified during the summer 2018 period which were mapped from remotely sensed data and provided by the Swedish Forest Agency (Skogsstyrelsen). Each 20×20 m^2 plot was located within

distinct burn scars (greater than 2 km separation) to reduce potential for pseudoreplication or spatial autocorrelation (Bataineh
90 et al., 2006) and allow for increased spread across the climate gradients (Schweiger et al., 2016). Remote sensed data was
taken as the average pixel value within a 20 m diameter circle centered on the plot with GIS analysis utilizing QGIS (QGIS
Development Team, 2019), ArcGIS (Esri Inc., 2019) and the pandas Python 3 package (Wes McKinney, 2010). The first
constraints on site selection were to avoid wetland or steeply sloping areas using prefire, topo-edaphic derived soil moisture
data (TEM) provided by the Swedish Environmental Protection Agency (Naturvårdsverket) (Naturvårdsverket, 2018) and
95 elevation and slope data provided within the ArcGIS software environment. This restricted the study to non-wetland ecosystem
types, which tend to have markedly differing ecosystem functioning than relatively dry forested regions, and to retain focus on
climate driven effects and their space-for-time substitution by reducing the effects of exogenous variables such as topography on
models. Next, sites with postfire salvage logging were omitted using recent visual imagery along with Swedish Forest Agency
records. Burnt plot selection was then filtered to maximize the spread over latitude, MAT and MAP gradients. Sentinel-2
100 infrared imagery taken during the time of fire assisted in delineating the exact locations of burnt plots by placing them where
there had been a strong and consistent infrared signal that was well within the mapped final fire boundaries. This gave greater
certainty of strong development of sustained fire. Manual assessment of visual and infrared imagery was performed through
the brandkarta web application provided by the Swedish Forest Agency.

Prefire properties of each burnt plot were estimated by measurements from a single identically sized adjacent control plot
105 centered between approximately 15 and 150 m outside the fire boundaries (100 plots total, i.e. 50 plot pairs). To reduce
mismatch between control and prefire burnt plot properties the following restrictions were placed on control plot selection.
Control plot locations were selected to minimize elevation, slope and TEM differences from the adjacent burnt plot. Swedish
Forest Agency data regarding tree species, overstory biomass, and basal area (collected during 2014) were used to best match
properties of control and burnt plot pairs. Stand appearance and age were examined with historic, visual images provided by
110 the Swedish National Land Survey (Lantmäteriet) verifying time since last disturbance had been at least 30 years for plot pairs
and that stand structure between plot pairs appeared physically connected over this period.

Due to their documented effects on emissions, long and short term approximations of moisture were introduced as exogenous
variables to models in order to test the ability of the study design to isolate variation in C and N stock losses to the effects
of climate. Long term moisture was represented by the TEM used in plot selection while short term moisture balance used
115 the Standardized Precipitation-Evapotranspiration Index (SPEI) over the period January to June 2018 (i.e. spei06 2018-06) to
capture the desiccation process leading up to the fire season. This variable was also compared to summer 2018 anomalies in
temperature and precipitation, i.e. the difference in the 2018 June, July, and August average of these values from those during
the same months averaged over the period from 1961 to 2017.

2.2 Sampling

120 Site visits occurred approximately 1 year postfire over the dates August 5 to August 20 in 2019. Sampling and analysis were
broken into six forest compartments. These were the four soil layers of mineral, duff, moss/litter and char as well as the
two aboveground compartments of the understory and overstory vegetation. The organic layer was considered the grouping

of the duff, moss/litter and char layers. Each compartment was further sorted by weight into characteristic features to form compartment compositional variables (CCVs) which were used in regression to test for relationships between compartment

125   composition and the quantity and quality of fuel loading as well as C and N loss.

2.2.1 Soil

Soil horizon depths (i.e. the distance from bottom to top of each individual layer) of the mineral, duff, moss/litter, and char layers were measured at 20 points per plot from 10 equally spaced excavations along each plot diagonal. The mineral layer was measured from its highest rock obtrusion to the bottom of the duff layer. The duff layer was considered the conglomer-

130   ate of the F (partially decomposed material) and H (humic material) layers in accordance with the Canadian system of soil classification (Canada Soil Survey Committee, 1978), as is common in boreal wildfire literature. The moss/litter layer was all unburnt material on top of the duff layer, including visually identifiable detritus and living moss. In all burnt sites, a layer of conglomerated char formed a clear boundary on top of the moss/litter allowing for distinct measurement. Here, char is defined as fully blackened, brittle material with apparent high heat exposure due to fire.

135   Samples were acquired for all four soil layers. Four mineral soil samples were taken using a 3 cm diameter corer at four corners of a square each 15 m from the plot center. Where feasible, 10 cm vertical mineral cores were taken, however in shallower layers a minimum depth of 5 cm each was collected. Duff samples were taken near the mineral cores by excavating four soil volumes (at least 400 cm^3 each) and trimming the mineral and moss/litter layers off the bottom and top of the volumes respectively. Duff and mineral soils were kept frozen until portions were freeze dried for separate analysis. Moss/litter samples

140   were collected at approximately equal intervals along the soil profile transects in a 553 cm^3 steel container with attention to preservation of the natural in situ volume. Char was similarly collected in a 112 cm^3 container. On the upper surface of the char layer were small portions of dry, unburnt material, much of which may be new additions of litter to the forest floor. This material was discarded from the char collection and was not included in stock estimates.

2.2.2 Vegetation

145   Individual tree bole diameter (sampled at 130 cm height above the forest floor) and species were recorded on site for all trees of at least 5 cm diameter at measurement height. If a fallen tree was charred only on its lower (in standing orientation) portions it was deemed standing during fire ignition and its measurements were included if its base was within plot boundaries. In burnt plots, the percentage of brown and black of each tree canopy was visually estimated and approximated as 0%, 25%, 50%, 75%, or 100%. Overstory biomass was calculated by entering bole diameters into allometric equations for Scots pine (*Pinus*

150   *sylvestris*), Norway spruce (*Picea abies*), silver birch (*Betula pendula*), and downy birch (*Betula pubescens*) (Marklund, 1987). The equations provided CCVs derived from biomass of stem wood, stem bark, living branches, dead branches, and stump for all species. Roots ≥ 5 cm diameter, roots < 5 cm diameter and needle biomass were additionally provided for pine and spruce. When testing the influence of overstory vegetation on C and N loss bole diameters from the burnt plots were used and not the adjacent control. C and N stock estimates for overstory were not included in analysis and its measurements were only used to

155   assess its role in controlling C and N stocks in all other compartments.

In all plots understory was clearly distinguished from overstory by pronounced height differences and samples were taken from control plots by cutting all non-moss, non-tree plant material at the surface of the soil from within four 40×40 cm^2 patches. Patches were chosen for their representativeness of plant abundance and composition for the portion of the plot that was vegetated, which was always all non bare rock surface. These values were applied to a visual estimate of non bare rock
160   surface area of the burnt plots as an approximation of its prefire understory coverage. CCVs for understory were determined by sorting the sampled understory plant material and measuring dried weights of the functional groups graminoid, forb, shrub, and pteridophyte.

2.3   Sample processing

All samples were dried at 40 °C for at least 3 days. Mineral and duff samples were sieved to 2 mm and 4 mm respectively.
165   CCVs for these two layers were formed by weights of these coarse and fine fractions. Dry moss/litter samples were weighed and visual estimates for percentage volume of needles, broad leaves, woody material, moss and lichen were multiplied by total weight to form CCVs. Bulk density of each soil layer per plot was calculated as the total dry weight of its samples divided by their total volume on collection. All samples were pulverized, except the mineral soil where only the fine earth fraction (< 2 mm) was analyzed (C and N content was set to 0 for the coarse fraction), and run through a Costech ECS4010
170   elemental analyzer to produce ratios of C and N weight to sample total weight (C_R and N_R respectively). Duff and mineral layer elemental weight ratios were recalculated by the sum of C or N in each of their fine and coarse fractions and divided by total compartment weight. The C:N ratio for each ecosystem compartment was calculated by dividing its total weight of C by total weight N.

2.4   Data analysis

175   Data was stored in comma-separated value files with minimal redundancy. Calculations were performed with custom written Python 3 code using the pandas library. The measurable properties used in stock calculation within soil compartments are the depth, bulk density and C_R or N_R. Total C and N stocks per soil compartment were calculated as a product of these properties using the equation

$$Stock_Z = d \cdot \rho \cdot Z_R \tag{1}$$

180   where subscript Z is substituted with C or N for reference to C or N stocks, d is the soil layer depth in meters, ρ is the layer bulk density (kg m^{-3}) and Z_R is C_R or N_R. Understory compartment stock calculations were performed with the equation

$$Stock_Z = \frac{m}{A} \cdot Z_R \cdot F \tag{2}$$

where m is the sampled mass in kilograms, A is sampled area (m^2), Z_R is C_R or N_R, and F is the estimated fractional vegetation coverage of the 20×20 m^2 plot.
185   Changes between control and burnt plots were first calculated by subtracting control plot values of a variable from those of its burnt pair thereby forming a single distribution of 50 elements for statistical testing. When C and N stocks were described

as losses their distribution was negated. These distributions were approximated as normal and unless otherwise noted all confidence intervals were constructed at the 95% level using the formula

$$I = \bar{x} \pm z \cdot \frac{\sigma}{\sqrt{n}} \tag{3}$$

where $\bar{x}$ is the sample mean, z is always 1.96 for the 95% interval, σ its standard deviation and n the sample size (always 50). Significance of differences between control and burnt plots was deemed to be when their interval did not include zero.

Simple regression was performed using the stats.linregress method from SciPy (Virtanen et al., 2020) providing significance (p), correlation (r), and slope (b). Multiple regression was carried out with the OLS method in the Python 3 statsmodels package (Seabold and Perktold, 2010) with models evaluated in order of increasing Akaike information criterion. Standardized regression coefficients (β) were produced by normalizing all variables (converting to z scores) before regression. CCVs were assessed in regression models both using original variables and their principal components produced by the PCA method in statsmodels. The effects of C and N stock arrangement amongst forest compartments was tested by entering the per plot ratios of the sums of different combinations of compartment stocks into regression analyses. Here, variables are considered correlated when p values from simple regression are less than 0.05.

Charting was performed using seaborn (Waskom and the seaborn development team, 2020) and Matplotlib (Hunter, 2007). Bar plot confidence intervals of the mean were bootstrapped at 95% and $n = 10,000$ using the seaborn.barplot method. Additional Python 3 packages that assisted in data exploration were NumPy (Harris et al., 2020) and pingouin (Vallat, 2018).

3   Results

3.1   C and N stock losses and rearrangement

Averaging across all sites sampled, fire caused significant rearrangement of C and N stocks particularly through changes in soil depth and bulk density which increased the mass per volume of both C and N. Significant decreases in total C stocks in burnt plots from their paired controls were observed, but changes in N were insignificant. Fire clearly transferred large amounts of C and N from lower soil layers to the highly nitrogenous surface layer of char. Organic layer C_R was unaffected by fire, however strong changes in N_R were measured resulting in an overall significant increase in the C:N ratio of this layer. Mean values and confidence intervals of the changes from control to burnt plots highlighted in this section for all compartments are found in Table 1 with soil specific properties found in Table 2.

The largest total loss of C in burnt plot compartments due to fire was from the duff layer (Fig. 2a). About three quarters of the moss/litter C was removed from burnt plots, comprising about half as much as the total amount of C that was removed from the duff layer. Understory C removal due to fire was near complete but had a relatively small contribution to overall elemental stocks and their changes. Of the average amount of C lost from these three compartments, 54.3% was found in the averaged char layer and only 0.19% in the increased C found in burnt plot mineral layers which themselves had no significant overall change in C between control and burnt plots.

Fire rearranged N significantly despite having no overall effect on its total amount (Fig. 2b). Similar percentages of N as C were lost from the duff, moss/litter and understory compartments with 100.8% of their averaged amount of lost N found in the
220 char layer and 5.1% in increased burnt plot mineral layer which itself had no significant change in total N.

Disproportionate changes of C and N from control to burnt plots caused significant decreases in the C:N ratio in all compartments except the duff layer which was unchanged (Fig. 2c). The low C:N ratio in the char layer (29.78 ± 1.70) made a strong contribution to the overall reduction in this value in burnt plot organic layers compared to control.

The duff layer C_R and N_R did not change significantly, though the moss/litter layer showed a significant increase in both val-
225 ues in burnt plots compared to their paired controls (Fig. 3c, 3d). These layers together with the char layer C_R (0.498 ± 0.0190) and N_R (0.0173 ± 0.00108) resulted in the organic layer having no change in C_R but a significant increase in N_R in burnt plots. The mineral layer experienced significant decreases of C_R and N_R in burnt plots both overall and in the fine fraction C_R (-0.0210 ± 0.0145, -33.7%) and N_R (-0.000509 ± 0.000415, -24.1%) compared to the controls.

Fire had a strong effect on reducing soil layer depths with removal of nearly the entire moss/litter layer and about one third
230 of the duff thickness (Fig. 3a). Together with the formation of the char layer and insignificant mineral layer depth changes, fire removed about a quarter of total soil depth and nearly 40% of the organic layer depth in burnt plots. Fire induced increases in bulk density of the soil layers counteracted C and N loss due to these depth changes (Fig. 3b). Bulk density of both the duff and moss/litter layers increased significantly and, along with producing a dense char layer, fire had a strong densifying effect on the organic layer.

235 To quantify the relative contribution of fire induced changes in organic layer depth, bulk density and elemental weight ratios on organic layer C and N losses they were linearly combined and entered into multiple regression. The C loss regression produced a model of fit of $R^2 = 0.865$ and standardized regression coefficients for changes in depth ($\beta = -0.670$), bulk density ($\beta = -0.633$) and C_R ($\beta = -0.583$). N loss produced a model fit of $R^2 = 0.777$ and coefficients for loss of depth ($\beta = -0.599$), bulk density ($\beta = -0.398$) and N_R ($\beta = -0.382$). This shows that changes of these variables due to fire all had a strong effect on
240 stock loss estimates. Measured change in organic layer depth is the strongest determinant of losses of N. However, for C bulk density and elemental weight ratios are nearly as important as depth.

3.2 Forest level drivers of fire induced C and N loss

The strongest correlator to total C and N losses among long term ecosystem properties was total paired control plot C ($p < 0.001$, $r = 0.703$, $b = 0.744$) and N stocks ($p < 0.001$, $r = 0.585$, $b = 0.574$), respectively. An even stronger correlation was found be-
245 tween control plot organic layer C and N stocks (here abbreviated C_O and N_O) and estimated losses of C ($p < 0.001$, $r = 0.736$, $b = 0.762$) and N ($p < 0.001$, $r = 0.653$, $b = 0.665$) from this compartment. Due to this increased explanatory power, and because the majority of fire affected stocks were located there, the focus of analysis was placed on the organic layer. Variables used in regression with percentage changes in C and N stocks tended to have less explanatory power than total stock losses and also were sensitive to outliers having erratic changes in model fit with removal of data points. Therefore only total stock losses
250 were assessed.

The interaction effect of C_O and N_O (i.e. its C:N ratio) was added to improve model fit. C_O and its C:N ratio strongly explained C_O losses ($p < 0.001$, $R^2 = 0.588$) while N_O and its C:N ratio explained N_O losses with slightly less strength ($p < 0.001$, $R^2 = 0.519$). Multicollinearity between the organic layer C:N ratio and C_O ($p = 0.003$, $r = -0.411$, $b = -1.96$ kgC/m^2) and N_O ($p < 0.001$, $r = -0.578$, $b = -92.2$ kgN/m^2) did not produce a high condition number in these models (1.55 for C, 1.93 for N) suggesting they are robust to these covariations (Alin, 2010).

Total char layer C was not significantly related to loss of C_O ($p = 0.137$) however a significant correlation using simple regression was found between char layer N and losses of N_O ($p = 0.011$, $r = -0.359$, $b = -0.838$). C_O loss was explained ($R^2 = 0.626$) by char C ($\beta = -0.199$) along with C_O ($\beta = 0.822$) and its C:N ratio ($\beta = 0.197$). Similarly, N_O loss was explained ($R^2 = 0.629$) by char N ($\beta = -0.347$) with N_O ($\beta = 0.824$) and its C:N ratio ($\beta = 0.254$).

CCVs and arrangement of C and N stocks amongst control plot compartments could not improve models explaining C_O and N_O losses in multiple regression with C_O and N_O respectively nor could they significantly explain the build up of organic layer fuel in control plots or production of char C or N. Relations either did not suitably meet the basic assumptions of regression, were deemed to be confounding or lacked supporting causal mechanism and were at a high risk of omitted-variable bias.

3.3 Climatic drivers of fire induced C and N loss

MAP had a directly proportional relation to both C_O ($p < 0.001$, $R^2 = 0.465$, $b = 0.0194$ $kgC/m^2/mm$) and N_O ($p = 0.012$, $R^2 = 0.352$, $b = 0.000416$ $kgN/m^2/mm$) losses. MAT was negatively quadratically related to losses in C_O ($p = 0.008$, $R^2 = 0.186$) and N_O ($p = 0.002$, $R^2 = 0.233$), both peaking near 4 °C. In multiple regression the MAT and MAT^2 terms lost significance and MAP was the dominant explaining factor of C_O and N_O losses. MAT and MAP were not significantly related in simple regression ($p = 0.829$) however a negative quadratic function of MAT in multiple regression explained MAP ($p < 0.001$, $R^2 = 0.407$), again peaking near 4 °C. This suggests that the direct climate dependence of C_O and N_O losses were driven by MAP, with MAT relating indirectly through its association to MAP.

C_O and N_O were broken down into the three measured aspects of depth, bulk density, and elemental weight ratio and entered as a linear combination in multiple regression within path analyses (Fig. 4a, b). MAT and MAP enhanced fire induced C_O and N_O loss by promoting development of a denser, more voluminous fuel load with additional direct effects on losses by MAT. MAT mitigates C_O loss by reducing C_R, however variation in this value does not affect C_O loss as strongly as depth and bulk density. Conversely, MAT promotes N_O loss through a higher N_R fuel but exerts a stronger direct effect on reduction of N_O removal due to fire than in the C_O model. Accordingly, a separate multiple regression showed strong negative effects of MAT and MAP on organic layer C:N ratio (Fig. 5a) as well as a direct effect of MAT ($p < 0.001$, $r = -0.568$, $b = -2.50$ °C^{-1}). CCVs could not strongly link MAT or MAP with C_R, N_R, or the C:N ratio in control plot organic layers.

Total char layer mass ($p < 0.001$, $r = 0.453$, $b = 0.316$ kg/m^2/°C) and char C_R ($p = 0.002$, $r = -0.435$, $b = -0.012$ °C^{-1}) were correlated with MAT but not the total mass of prefire fuel. This means that warmer regions produced larger amounts of lower C_R material irrespective of total fuel amount. In a multiple regression using C_O, the organic layer C:N ratio, MAT, MAP and total char layer C production to explain C_O loss, direct effects of MAT lost significance and overall model fit was improved (Fig. 5a). This suggested that, while controlling for C_O and the organic layer C:N ratio, C_O loss from this layer was

285   reduced by MAT through the creation of char. Similarly, N_O loss is further explained by additions of char layer N to the climate model but a large direct effect of MAT remains (Fig. 5b). The organic layer C:N ratio in the N model was able to replace the direct effect of MAT, however with decreased model fit and inflation of variables which is suggestive of a confounding influence of the organic layer C:N ratio on MAT and N_O loss. Again, CCVs and fuel arrangement could not improve either model.

3.4   Moisture and summer 2018 anomalies

290   TEM in control plots was not directly related to C_O ($p = 0.248$) or N_O ($p = 0.259$) stocks though it slightly improved model fit when joined with MAT and MAP in explaining these variables (Fig. 5a, b). TEM differences between paired burnt and control plots were observed to increase both with control and burnt TEM levels however not along gradients of MAT ($p = 0.198$), MAP ($p = 0.771$), C_O ($p = 0.302$) or N_O ($p = 0.423$). TEM differences between paired burnt and control plots were entered into simple regression with losses in C_O ($p = 0.088$, $r = -0.244$, $b = -0.0132$ kgC/m^2) and N_O ($p = 0.035$, $r = -0.299$,

295   $b = 0.00415$ kgN/m^2). Although, correction for these slopes by using non-standardized coefficients of regression for TEM, MAT and MAP against C_O and N_O produced no significant change in losses of C_O or N_O.

    SPEI was related to MAT ($p < 0.001$, $r = -0.869$), temperature anomaly ($p < 0.001$, $r = -0.892$), precipitation anomaly ($p = 0.002$, $r = -0.433$) but not to MAP ($p = 0.725$), or losses of C_O ($p = 0.712$) and N_O ($p = 0.644$) due to fire. When included in multiple regression with MAP, MAT, char C or N, and C_O or N_O to explain fire induced C_O or N_O stock losses, respectively, SPEI

300   either did not improve model fit or promoted high uncertainty of variables. SPEI was directly related to char C ($p = 0.013$, $r = -0.348$) and N ($p = 0.012$, $r = -0.351$) but had high uncertainty when explaining these variables in multiple regression with MAT which suggests SPEI is a confounding variable. Additionally, anomalies of temperature ($p < 0.001$, $r = 0.956$) and precipitation ($p < 0.001$, $r = -0.525$) were strongly correlated to their respective long term values with the temperature anomaly offering improved explanation of total char production ($p < 0.001$, $r = 0.477$, $b = 0.179$ kg/m^2/°C) over MAT.

305 ## 4   Discussion

4.1   Trends in ecosystem C and N stocks

Significant overall reduction in C stocks were found in burnt plots relative to their paired control, with the largest removals from the duff layer. Averaged total C loss was relatively low at 0.815 ± 0.652 kgC/m^2 (15.6%) compared to estimates from inland Alaskan black spruce stands (3.3 kgC/m^2) (Boby et al., 2010) but was comparable to averaged losses from Scots pine

310   stands in Siberia (0.992 kgC/m^2) (Ivanova et al., 2011). However, N stocks were not significantly different overall in burnt plots compared to controls. This contrasts with the Alaskan study which estimated percentage removal from soils of N (49.8%) to be similar to C (52.9%) at an average loss of 0.09 kgN/m^2 (Boby et al., 2010). Averaging over the 50 burnt plots, N was clearly removed in large amounts from the duff and moss/litter layers but its transfer into a highly nitrogenous char layer prevented differences when considering the overall soil profile. The char layer was likely largely produced by fire interacting

315   with the understory and moss/litter layer, however averaged char layer C and N stocks were greater than losses from the two

layers combined suggesting large contributions also from the duff layer. In burnt plots with residual moss/litter an upwards mixing of mobilized duff C and N may have occurred due to simultaneous effects of heating throughout the depth of the fuel bed. Because the char layer was conglomerated and completely blackened it is unlikely that material was incorporated postfire. However, material may have been added from downward movement of overstory components during the time of fire. The above

320 mentioned study in Alaskan black spruce forests, which are known for their great extent of canopy damage (Walker et al., 2020; Boby et al., 2010), showed C and N loss from the canopy to be about an order of magnitude lower than losses from soil while also assuming that losses from the tree bole are negligible and that a large fraction of these overstory losses were released to the atmosphere (Boby et al., 2010). In the current study, low levels of overstory damage and its lack of correlation with char layer mass suggests that the large majority of C and N stock changes between control and burnt plots were captured within the

325 sampled soil and understory compartments.

The lack of change in total N stock due to fire is consistent with available evidence from existing study in Fennoscandian forests where fire had only slight effects on total N over extended periods (Palviainen et al., 2017). N losses in non-boreal forests have been related to fuel temperature during time of fire with lower intensity fires transferring a greater proportion of pools of organic N into soil ammonium and nitrate rather than removing N in gaseous forms (Neary et al., 1999). Laboratory studies

330 have linked the amount of N transferred from organic to inorganic forms during heat exposure to both applied temperature and fuel type (Gundale and DeLuca, 2006; Makoto et al., 2011). Therefore, the N cycle in boreal systems may be highly dependent on active fire properties, fuel type and resulting fuel transformation and the greater N losses in Alaska compared to Eurasia could be explained by its dissimilar fuel and the characteristically more intense fires across the North American boreal zone (de Groot et al., 2013a; Wooster and Zhang, 2004). Fire intensity and temperature may also be related to C losses

335 and overall fuel transformation, so it is of interest to compare remote measurements (i.e. satellite data) of these time-of-fire properties to on-site measured ecosystem changes. This can lead to a more complete predictive understanding of wildfire in the entire Fennoscandian region and beyond.

In addition to removals, C and N was densified by fire in the organic layer due to significant drops in depth and increased bulk density in burnt plots. Mean C_R dropped in duff between plot pairs driven most likely by the increased ratio of incombustible

340 inorganic material to remaining organic material. However, increased variability of duff C_R in burnt plots contributed to the insignificance of this change and appeared to be related to extreme volume reductions which reduced the duff layer to exceptionally ashy, rocky material in some plots. C_R and the C:N ratio in the char layer measured here are surprisingly low compared to known measurements showing char to be highly carbonaceous with C:N ratios often well above 100 (Hart and Luckai, 2014). Fire induced structural change of fuel has been shown to play a strong role in N retention where highly

345 porous char material adsorbs inorganic N preventing its leaching loss from the system until its reuptake into organic forms by plants or microbes (Makoto et al., 2012). This sorptive power has been observed to fade over the interval between fire events suggesting newly produced char is required for this retention effect (Zackrisson et al., 1996). The high nitrogen content of the char layer may therefore be due to adsorption of fire mineralized N and act as a steady source of bioavailable nutrients to plant and microbial communities during succession. This study employed coarse-scale sampling of char based on soil horizon

350 identification and separation in the field and a more rigorously defined assessment of char production in all layers may provide
more detailed relations to climate and soil processes.

4.2   Climate linked effects of fire

Both MAP and MAT had significant direct relations to total C and N removals from plots with the strongest mediator being
estimated prefire C and N stocks in the organic layer. MAP had a stronger effect on the build up of control plot fuel, namely

355 through a positive correlation with total organic layer depth. MAT affected C and N losses through increasing bulk density,
reducing C_R and increasing N_R thus reducing the C:N ratio in the organic layer in control plots, suggesting warmer conditions
had a fuel conditioning effect through greater decomposition of organic soils (Callesen et al., 2007). When controlling for
control plot organic layer C and N stocks and their ratios using multiple regression, MAT had a direct negative effect on C and
N losses from this layer. This direct effect was largely mediated by incorporation of measures of fire induced fuel transformation

360 into the models, i.e. production of char layer C or N. These models suggest that warmer regions tended to conserve larger pools
of fire affected fuel as charred material rather than release it from the ecosystem either in gaseous or dissolved forms. This
fuel transformation in turn may have extended effects on C and N turnover through links to nutrient availability and the biotic
community which in turn affect process rates such as primary production and soil decomposition (Schmidt and Noack, 2000).

4.3   Considering representativeness and prediction of future wildfire impacts

365 Ignition probability and fire propagability may relate to the analyzed drivers in this study with ignition and propagation more
likely in stands with greater and more flammable fuel loads. As a result, C and N losses might have been underestimated by
burnt plots being biased to a greater prefire fuel load than their paired controls (systematic error) rather than these differences
being approximately random (random error). This was evident in the fact that N losses were centered near 0 by their mean yet
had a strong correlation with control plot total N despite the improbability that fire actually increased total N within nearly half

370 of the burnt plot sample pool. Contrarily, control plots were biased towards higher TEM, which was observed to be related to
greater fuel loading in measured control plots, though the magnitude of this bias did not increase along gradients of climate
or fuel loading nor did attempts to correct for it significantly affect C and N loss estimates. Therefore, control plot matching
appears to have been performed adequately within the scope of data collected with any potential bias coming from unknown
parameters. Further investigation of these parameters is merited in order to improve control plot matching methodology and

375 better constrain emission estimates in this region.

Variation of many ecosystem properties could not be statistically linked to C and N losses, though that does not mean they are
without role in determining extent of emissions and ecosystem change. Cross regional boreal wildfire study has shown variables
such as the abundance of spruce to strongly affect C emissions across regions, but within a single region the abundance may be
too homogeneous to show an effect (Walker et al., 2020). Furthermore, ratios of fine to heavy fuel loads have been manipulated

380 in experimental burns to produce varying fire severity (Alexander et al., 2018; Ludwig et al., 2018). Accordingly, CCVs and
fuel arrangement amongst compartments in this study may have been simply too homogeneous to produce significant results

but may nevertheless still provide valuable statistical signals for understanding drivers of fire processes across regions and fire severities.

Previous studies have demonstrated strong effects of moisture on boreal wildfire C emissions. For example, a study including 385 several large North American fire complexes found C emissions to increase along gradients of topo-edaphic derived soil moisture (due to its positive relation to total fuel) until reaching high moisture sites where the trend inverted and began to decrease due to the inhibiting effects of this increased moisture on fuel availability (Walker et al., 2018). The position of this point of inflection along the long term moisture curve is likely dictated by short term moisture levels, which are in turn controlled by the extremity of drying during a fire season. Accordingly, fuel availability, and therefore C emissions, are strongly 390 dependent on drying processes specific to individual stand composition and structure and its local fire weather. By incorporating measures of long and short term moisture balance, climate based path models gained only slight improvements in explaining fuel build up and no increased explanatory power regarding C and N losses. Therefore, the study design distinguished climate driven effects on fire severity with only minimal restrictions on site selection (non-sloping, non-wetland) thereby providing results that are generally representative for Fennoscandian, non-wetland forests under similar drought conditions of summer 395 2018. However, with its strong correlations to drought indices, anomalies of temperature and precipitation as well as fuel charring and remaining direct effects on emissions, more remains to be understood about how MAT (and in addition, intra-annual distribution of MAP) relates to the fire regime across the conditions of different fire seasons.

Boreal wildfire literature has tended to focus on highly flammable forest ecosystems with intense burning of several hundred hectares or more despite the vast majority of fires in the boreal region being less than 200 ha (Stocks et al., 2002; Valendik, 400 1996). This research bias may limit knowledge to a particular population by studying fire events only at their utmost extremes and effectively masking important signals of ecosystem heterogeneity on fire severity at differing intensities. The only restriction this study placed on wildfire intensity and size was that the fire activity could be remotely confirmed using Sentinel-2 infrared data. This has the potential to affect comparability of results both in terms of total C and N losses as well as their drivers which may exhibit differing patterns and strengths over ranges of fire intensity. It may therefore be beneficial for wild-405 fire studies to be examined and compared within categories of absolute severity and intensity. This methodology might be particularly useful in gaining understanding of the drivers of fire severity as it increases in traditionally fire protected ecosystems such as wetlands (Zoltai et al., 1998), which tend to store vastly larger amounts of C per area than their dryer forested counterparts (Deluca and Boisvenue, 2012).

5 Conclusions

410 This study measured wildfire impacts across current climatic gradients of precipitation and temperature to show that climate controls total releases of C and N during fire events mainly due to its effect on increasing organic layer fuel load. The role of MAP is focused on the total quantity of this fuel load whereas MAT has a more qualitative effect by influencing bulk density, C_R and N_R in the organic layer. When controlling for total organic layer fuel, increasing MAT, and to a lesser extent MAP, reduces C loss due to fire through preconditioning of the organic layer as measured by a lowered C:N ratio. Additionally, both C and

415 N losses are mitigated by increased MAT through the sequestering of fire affected fuel into a surface layer of charred material. This conservation effect is stronger for N, which had no overall significant loss in stocks due to fire, and which also had stronger unexplained direct mitigating effects of MAT on its loss that were hypothesized to be related to time-of-fire properties such as fire intensity and temperature. While remaining ecosystem variables regarding fuel composition and arrangement could not be strongly linked to total C and N losses it is of interest to analyze their role in cross-regional comparisons and to investigate 420 whether they influence other fire related properties such as ignition likelihood, fire propagability and intensity. Advancing knowledge of the intricate ties between instantaneous processes of fire events and their long term effects on C and N cycling demands comprehensive research approaches that pay particular attention to climate sensitivity. This knowledge is imperative for producing accurate predictions of boreal forest functioning under future climate scenarios.

Data availability. All data used to produce the results in this document are original unless otherwise stated in the text. It is found freely 425 available through Eckdahl et al. (2021).

Author contributions. Author contributions using the CRediT contributor roles taxonomy are as follows: conceptualization (JE, JK, DB), data curation (JE), formal analysis (JE), funding acquisition (JK, DB), investigation (JE, JK, DB), methodology (JE, JK, DB), project administration (JE, JK, DB), resources (JE, DB), software (JE), supervision (JE, JK, DB), validation (JE, JK, DB), visualization (JE), writing – original draft preparation (JE), and writing – review & editing (JE, JK, DB).

430 *Competing interests.* The authors declare that they have no conflict of interest.

Acknowledgements. JAE was supported by the strategic research area Biodiversity and Ecosystems in a Changing Climate, BECC, at Lund University. JAK was supported by the Carlsberg Foundation (grant CF20-0238). C and N analyses were performed in the Department of Geology, Lund University under supervision of Karl Ljung. Valuable information was provided by representatives from the Swedish Forest Agency (Skogsstyrelsen) and Swedish Civil Contingencies Agency (Myndigheten för samhällsskydd och beredskap, MSB). Thank you to 435 Geerte de Jong for dedicated assistance in field work planning and execution. Crucial field and lab assistance was provided by Rieke Madsen, Femke Pijcke, Lotte Wendt, Julia Iwan, and Henni Ylänne. Guidance from Karl Ljung, Åsa Wallin, Patrik Vestin and Michael Gundale in sample collection and processing was critical and highly appreciated. Friends, family, and colleagues were vital sources of support and inspiration throughout this work.

References

440 Alexander, H. D., Natali, S. M., Loranty, M. M., Ludwig, S. M., Spektor, V. V., Davydov, S., Zimov, N., Trujillo, I., and Mack, M. C.:
Impacts of increased soil burn severity on larch forest regeneration on permafrost soils of far northeastern Siberia, Forest Ecology and
Management, 417, 144–153, https://doi.org/10.1016/j.foreco.2018.03.008, 2018.

Alin, A.: Multicollinearity, WIREs Computational Statistics, 2, 370–374, https://doi.org/10.1002/wics.84, 2010.

Bataineh, A. L., Oswald, B. P., Bataineh, M., Unger, D., Hung, I.-K., and Scognamillo, D.: Spatial autocorrelation and pseudoreplication in
445 fire ecology, Fire Ecology, 2, 107–118, https://doi.org/10.4996/fireecology.0202107, 2006.

Boby, L. A., Schuur, E. A. G., Mack, M. C., Verbyla, D., and Johnstone, J. F.: Quantifying fire severity, carbon, and nitrogen emissions in
Alaska's boreal forest, Ecological Applications, 20, 1633–1647, https://doi.org/10.1890/08-2295.1, 2010.

Bond-Lamberty, B., Peckham, S. D., Ahl, D. E., and Gower, S. T.: Fire as the dominant driver of central Canadian boreal forest carbon
balance, Nature, 450, 89–92, https://doi.org/10.1038/nature06272, 2007.

450 Callesen, I., Raulund-Rasmussen, K., Westman, C., and Tau-Strand, L.: Nitrogen pools and C:N ratios in well-drained Nordic forest soils
related to climate and soil texture, Boreal Environment Research, 12, 681–692, 2007.

Canada Soil Survey Committee: The Canadian system of soil classification, Research Branch, Canada Department of Agriculture, 1978.

Certini, G.: Effects of fire on properties of forest soils: a review, Oecologia, 143, 1–10, https://doi.org/10.1007/s00442-004-1788-8, 2005.

De Frenne, P., Graae, B. J., Rodríguez-Sánchez, F., Kolb, A., Chabrerie, O., Decocq, G., De Kort, H., De Schrijver, A., Diekmann, M.,
455 Eriksson, O., Gruwez, R., Hermy, M., Lenoir, J., Plue, J., Coomes, D. A., and Verheyen, K.: Latitudinal gradients as natural laboratories
to infer species' responses to temperature, Journal of Ecology, 101, 784–795, https://doi.org/10.1111/1365-2745.12074, 2013.

de Groot, W., Bothwell, P., Carlsson, D., and Logan, K.: Simulating the effects of future fire regimes on western Canadian boreal forests,
Journal of Vegetation Science, 14, 355–364, https://doi.org/10.1111/j.1654-1103.2003.tb02161.x, 2003.

de Groot, W. J., Cantin, A. S., Flannigan, M. D., Soja, A. J., Gowman, L. M., and Newbery, A.: A comparison of Canadian and Russian
460 boreal forest fire regimes, Forest Ecology and Management, 294, 23–34, https://doi.org/10.1016/j.foreco.2012.07.033, 2013a.

de Groot, W. J., Flannigan, M. D., and Cantin, A. S.: Climate change impacts on future boreal fire regimes, Forest Ecology and Management,
294, 35–44, https://doi.org/10.1016/j.foreco.2012.09.027, 2013b.

Deluca, T. H. and Boisvenue, C.: Boreal forest soil carbon: distribution, function and modelling, Forestry, 85, 161–184, https://doi.org/10.
1093/forestry/cps003, 2012.

465 Eckdahl, J., Kristensen, J., and Metcalfe, D.: Dataset for Boreal Forest Wildfire and Climate Linked Drivers of Carbon and Nitrogen Loss,
https://doi.org/10.5281/zenodo.5078669, 2021.

Esri Inc.: ArcGIS Pro, Esri Inc., https://www.esri.com/en-us/arcgis/products/arcgis-pro/, 2019.

French, N. H., Goovaerts, P., and Kasischke, E. S.: Uncertainty in estimating carbon emissions from boreal forest fires, Journal of Geophysical
Research: Atmospheres, 109, https://doi.org/10.1029/2003JD003635, 2004.

470 Gaboriau, D. M., Remy, C. C., Girardin, M. P., Asselin, H., Hély, C., Bergeron, Y., and Ali, A. A.: Temperature and fuel availability
control fire size/severity in the boreal forest of central Northwest Territories, Canada, Quaternary Science Reviews, 250, 106 697, https:
//doi.org/10.1016/j.quascirev.2020.106697, 2020.

Gillett, N., Weaver, A., Zwiers, F., and Flannigan, M.: Detecting the effect of climate change on Canadian forest fires, Geophysical Research
Letters, 31, https://doi.org/10.1029/2004GL020876, 2004.

Gundale, M. J. and DeLuca, T. H.: Temperature and source material influence ecological attributes of ponderosa pine and Douglas-fir charcoal, Forest ecology and management, 231, 86–93, https://doi.org/10.1016/j.foreco.2006.05.004, 2006.

Harris, C. R., Millman, K. J., van der Walt, S. J., Gommers, R., Virtanen, P., Cournapeau, D., Wieser, E., Taylor, J., Berg, S., Smith, N. J., Kern, R., Picus, M., Hoyer, S., van Kerkwijk, M. H., Brett, M., Haldane, A., Fernández del Río, J., Wiebe, M., Peterson, P., Gérard-Marchant, P., Sheppard, K., Reddy, T., Weckesser, W., Abbasi, H., Gohlke, C., and Oliphant, T. E.: Array programming with NumPy, Nature, 585, 357–362, https://doi.org/10.1038/s41586-020-2649-2, 2020.

Hart, S. and Luckai, N.: Charcoal carbon pool in North American boreal forests, Ecosphere, 5, 1–14, https://doi.org/10.1890/ES13-00086.1, 2014.

Hunter, J. D.: Matplotlib: A 2D graphics environment, Computing in Science & Engineering, 9, 90–95, https://doi.org/10.1109/MCSE.2007.55, 2007.

Ivanova, G., Conard, S., Kukavskaya, E., and McRae, D.: Fire impact on carbon storage in light conifer forests of the Lower Angara region, Siberia, Environmental Research Letters, 6, 045 203, https://doi.org/10.1088/1748-9326/6/4/045203, 2011.

Johnstone, J., Celis, G., Chapin III, F., Hollingsworth, T., Jean, M., and Mack, M.: Factors shaping alternate successional trajectories in burned black spruce forests of Alaska, Ecosphere, 11, e03 129, https://doi.org/10.1002/ecs2.3129, 2020.

Kasischke, E. S., Hyer, E. J., Novelli, P. C., Bruhwiler, L. P., French, N. H., Sukhinin, A. I., Hewson, J. H., and Stocks, B. J.: Influences of boreal fire emissions on Northern Hemisphere atmospheric carbon and carbon monoxide, Global Biogeochemical Cycles, 19, https://doi.org/10.1029/2004GB002300, 2005.

Kelly, R., Chipman, M. L., Higuera, P. E., Stefanova, I., Brubaker, L. B., and Hu, F. S.: Recent burning of boreal forests exceeds fire regime limits of the past 10,000 years, Proceedings of the National Academy of Sciences, 110, 13 055–13 060, https://doi.org/10.1073/pnas.1305069110, 2013.

Kohl, L., Philben, M., Edwards, K. A., Podrebarac, F. A., Warren, J., and Ziegler, S. E.: The origin of soil organic matter controls its composition and bioreactivity across a mesic boreal forest latitudinal gradient, Global Change Biology, 24, e458–e473, https://doi.org/10.1111/gcb.13887, 2018.

Lemprière, T., Kurz, W., Hogg, E., Schmoll, C., Rampley, G., Yemshanov, D., McKenney, D., Gilsenan, R., Beatch, A., Blain, D., Bhatti, J., and Krcmar, E.: Canadian boreal forests and climate change mitigation, Environmental Reviews, 21, 293–321, https://doi.org/10.1139/er-2013-0039, 2013.

Li, F., Lawrence, D. M., and Bond-Lamberty, B.: Impact of fire on global land surface air temperature and energy budget for the 20th century due to changes within ecosystems, Environmental Research Letters, 12, 044 014, https://doi.org/10.1088/1748-9326/aa6685, 2017.

Ludwig, S. M., Alexander, H. D., Kielland, K., Mann, P. J., Natali, S. M., and Ruess, R. W.: Fire severity effects on soil carbon and nutrients and microbial processes in a Siberian larch forest, Global Change Biology, 24, 5841–5852, http://dx.doi.org/10.1111/gcb.14455, 2018.

Makoto, K., Choi, D., Hashidoko, Y., and Koike, T.: The growth of Larix gmelinii seedlings as affected by charcoal produced at two different temperatures, Biology and Fertility of Soils, 47, 467–472, https://doi.org/10.1007/s00374-010-0518-0, 2011.

Makoto, K., Shibata, H., Kim, Y., Satomura, T., Takagi, K., Nomura, M., Satoh, F., and Koike, T.: Contribution of charcoal to short-term nutrient dynamics after surface fire in the humus layer of a dwarf bamboo-dominated forest, Biology and Fertility of Soils, 48, 569–577, https://doi.org/10.1007/s00374-011-0657-y, 2012.

Malhi, Y., Baldocchi, D., and Jarvis, P.: The carbon balance of tropical, temperate and boreal forests, Plant, Cell & Environment, 22, 715–740, https://doi.org/10.1046/j.1365-3040.1999.00453.x, 1999.

Marklund, L.: Biomass functions for Norway spruce (Picea abies (L.) Karst.) in Sweden [biomass determination, dry weight], Rapport-Sveriges Lantbruksuniversitet, Institutionen foer Skogstaxering (Sweden), 1987.

515   Mekonnen, Z. A., Riley, W. J., Randerson, J. T., Grant, R. F., and Rogers, B. M.: Expansion of high-latitude deciduous forests driven by interactions between climate warming and fire, Nature plants, 5, 952–958, https://doi.org/10.1038/s41477-019-0495-8, 2019.

Naturvårdsverket: Markfuktighetsindex producerat som del av Nationella marktäckedata, NMD, https://metadatakatalogen.naturvardsverket.se/metadatakatalogen/GetMetaDataById?id=cae71f45-b463-447f-804f-2847869b19b0, 2018.

Neary, D. G., Klopatek, C. C., DeBano, L. F., and Ffolliott, P. F.: Fire effects on belowground sustainability: a review and synthesis, Forest ecology and management, 122, 51–71, https://doi.org/10.1016/S0378-1127(99)00032-8, 1999.

520   Neff, J., Harden, J., and Gleixner, G.: Fire effects on soil organic matter content, composition, and nutrients in boreal interior Alaska, Canadian Journal of Forest Research, 35, 2178–2187, https://doi.org/10.1139/x05-154, 2005.

Palviainen, M., Pumpanen, J., Berninger, F., Ritala, K., Duan, B., Heinonsalo, J., Sun, H., Köster, E., and Köster, K.: Nitrogen balance along a northern boreal forest fire chronosequence, PloS one, 12, https://doi.org/10.1371/journal.pone.0174720, 2017.

Preston, C. M. and Schmidt, M. W.: Black (pyrogenic) carbon: a synthesis of current knowledge and uncertainties with special consideration

525   of boreal regions, Biogeosciences, 3, 397–420, https://doi.org/10.5194/bg-3-397-2006, 2006.

QGIS Development Team: QGIS Geographic Information System, QGIS Association, https://www.qgis.org, 2019.

Rabin, S. S., Melton, J. R., Lasslop, G., Bachelet, D., Forrest, M., Hantson, S., Kaplan, J. O., Li, F., Mangeon, S., Ward, D. S., Yue, C., Arora, V. K., Hickler, T., Kloster, S., Knorr, W., Nieradzik, L., Spessa, A., Folberth, G. A., Sheehan, T., Voulgarakis, A., Kelley, D. I., Prentice, I. C., Sitch, S., Harrison, S., and Arneth, A.: The Fire Modeling Intercomparison Project (FireMIP), phase 1: experimental

530   and analytical protocols with detailed model descriptions, Geoscientific Model Development, 10, 1175–1197, https://doi.org/10.5194/gmd-10-1175-2017, 2017.

Rapalee, G., Trumbore, S. E., Davidson, E. A., Harden, J. W., and Veldhuis, H.: Soil carbon stocks and their rates of accumulation and loss in a boreal forest landscape, Global Biogeochemical Cycles, 12, 687–701, https://doi.org/10.1029/98GB02336, 1998.

Rogers, B. M., Soja, A. J., Goulden, M. L., and Randerson, J. T.: Influence of tree species on continental differences in boreal fires and

535   climate feedbacks, Nature Geoscience, 8, 228–234, https://doi.org/10.1038/ngeo2352, 2015.

Ruiz, J. A. M., Riaño, D., Arbelo, M., French, N. H., Ustin, S. L., and Whiting, M. L.: Burned area mapping time series in Canada (1984–1999) from NOAA-AVHRR LTDR: A comparison with other remote sensing products and fire perimeters, Remote Sensing of Environment, 117, 407–414, https://doi.org/10.1016/j.rse.2011.10.017, 2012.

Schmidt, M. W. and Noack, A. G.: Black carbon in soils and sediments: analysis, distribution, implications, and current challenges, Global

540   biogeochemical cycles, 14, 777–793, https://doi.org/10.1029/1999GB001208, 2000.

Schultz, M. G., Heil, A., Hoelzemann, J. J., Spessa, A., Thonicke, K., Goldammer, J. G., Held, A. C., Pereira, J. M. C., and van het Bolscher, M.: Global wildland fire emissions from 1960 to 2000, Global Biogeochemical Cycles, 22, https://doi.org/10.1029/2007GB003031, 2008.

Schweiger, A. H., Irl, S. D. H., Steinbauer, M. J., Dengler, J., and Beierkuhnlein, C.: Optimizing sampling approaches along ecological gradients, Methods in Ecology and Evolution, 7, 463–471, https://doi.org/10.1111/2041-210X.12495, 2016.

545   Seabold, S. and Perktold, J.: statsmodels: Econometric and statistical modeling with python, in: 9th Python in Science Conference, http://dx.doi.org/10.25080/Majora-92bf1922-011, 2010.

Soja, A. J., Cofer, W. R., Shugart, H. H., Sukhinin, A. I., Stackhouse, P. W., McRae, D. J., and Conard, S. G.: Estimating fire emissions and disparities in boreal Siberia (1998–2002), Journal of Geophysical Research: Atmospheres, 109, https://doi.org/10.1029/2004JD004570, 2004.

550 Stocks, B. J., Mason, J. A., Todd, J. B., Bosch, E. M., Wotton, B. M., Amiro, B. D., Flannigan, M. D., Hirsch, K. G., Logan, K. A., Martell, D. L., and Skinner, W. R.: Large forest fires in Canada, 1959–1997, Journal of Geophysical Research: Atmospheres, 107, FFR 5–1–FFR 5–12, https://doi.org/10.1029/2001JD000484, 2002.

Tagesson, T., Schurgers, G., Horion, S., Ciais, P., Tian, F., Brandt, M., Ahlström, A., Wigneron, J.-P., Ardö, J., Olin, S., Fan, L., Wu, Z., and Fensholt, R.: Recent divergence in the contributions of tropical and boreal forests to the terrestrial carbon sink, Nature Ecology and
555 Evolution, 4, https://doi.org/10.1038/s41559-019-1090-0, 2020.

Valendik, E.: Temporal and spatial distribution of forest fires in Siberia, in: Fire in Ecosystems of Boreal Eurasia, pp. 129–138, Springer, https://doi.org/10.1007/978-94-015-8737-2_9, 1996.

Vallat, R.: Pingouin: statistics in Python, The Journal of Open Source Software, 3, 1026, https://doi.org/10.21105/joss.01026, 2018.

van Leeuwen, T. T., van der Werf, G. R., Hoffmann, A. A., Detmers, R. G., Rücker, G., French, N. H. F., Archibald, S., Carvalho Jr., J. A.,
560 Cook, G. D., de Groot, W. J., Hély, C., Kasischke, E. S., Kloster, S., McCarty, J. L., Pettinari, M. L., Savadogo, P., Alvarado, E. C., Boschetti, L., Manuri, S., Meyer, C. P., Siegert, F., Trollope, L. A., and Trollope, W. S. W.: Biomass burning fuel consumption rates: a field measurement database, Biogeosciences, 11, 7305–7329, https://doi.org/10.5194/bg-11-7305-2014, 2014.

Van Wagner, C.: Development and structure of the canadian forest fire weather index system, in: Can. For. Serv., Forestry Tech. Rep, Citeseer, 1987.

565 Vanhala, P., Karhu, K., Tuomi, M., Björklöf, K., Fritze, H., and Liski, J.: Temperature sensitivity of soil organic matter decomposition in southern and northern areas of the boreal forest zone, Soil biology and biochemistry, 40, 1758–1764, https://doi.org/10.1016/j.soilbio.2008.02.021, 2008.

Virtanen, P., Gommers, R., Oliphant, T. E., Haberland, M., Reddy, T., Cournapeau, D., Burovski, E., Peterson, P., Weckesser, W., Bright, J., van der Walt, S. J., Brett, M., Wilson, J., Millman, K. J., Mayorov, N., Nelson, A. R. J., Jones, E., Kern, R., Larson, E., Carey, C. J., Polat,
570 İ., Feng, Y., Moore, E. W., VanderPlas, J., Laxalde, D., Perktold, J., Cimrman, R., Henriksen, I., Quintero, E. A., Harris, C. R., Archibald, A. M., Ribeiro, A. H., Pedregosa, F., van Mulbregt, P., and SciPy 1.0 Contributors: SciPy 1.0: Fundamental Algorithms for Scientific Computing in Python, Nature Methods, 17, 261–272, https://doi.org/10.1038/s41592-019-0686-2, 2020.

Walker, X., Rogers, B., Veraverbeke, S., Johnstone, J., Baltzer, J., Barrett, K., Bourgeau-Chavez, L., Day, N., Groot, W., Dieleman, C., Goetz, S., Hoy, E., Jenkins, L., Kane, E., Parisien, M.-A., Potter, S., Schuur, E., Turetsky, M., Whitman, E., and Mack, M.: Fuel avail-
575 ability not fire weather controls boreal wildfire severity and carbon emissions, Nature Climate Change, pp. 1–7, https://doi.org/10.1038/s41558-020-00920-8, 2020.

Walker, X. J., Rogers, B. M., Baltzer, J. L., Cumming, S. G., Day, N. J., Goetz, S. J., Johnstone, J. F., Schuur, E. A. G., Turetsky, M. R., and Mack, M. C.: Cross-scale controls on carbon emissions from boreal forest megafires, Global Change Biology, 24, 4251–4265, https://doi.org/10.1111/gcb.14287, 2018.

580 Waskom, M. and the seaborn development team: mwaskom/seaborn, Zenodo, https://doi.org/10.5281/zenodo.592845, 2020.

Wes McKinney: Data Structures for Statistical Computing in Python, in: Proceedings of the 9th Python in Science Conference, edited by Stéfan van der Walt and Jarrod Millman, pp. 56 – 61, https://doi.org/10.25080/Majora-92bf1922-00a, 2010.

Wiggins, E. B., Andrews, A., Sweeney, C., Miller, J. B., Miller, C. E., Veraverbeke, S., Commane, R., Wofsy, S., Henderson, J. M., and Randerson, J. T.: Evidence for a larger contribution of smoldering combustion to boreal forest fire emissions from tower observations in
585 Alaska, Atmospheric Chemistry and Physics Discussions, 2020, 1–26, https://doi.org/10.5194/acp-2019-1067, 2020.

Wooster, M. J. and Zhang, Y. H.: Boreal forest fires burn less intensely in Russia than in North America, Geophysical Research Letters, 31, https://doi.org/10.1029/2004GL020805, 2004.

Zackrisson, O., Nilsson, M.-C., and Wardle, D. A.: Key ecological function of charcoal from wildfire in the Boreal forest, Oikos, pp. 10–19, https://doi.org/10.2307/3545580, 1996.

590 Zoltai, S., Morrissey, L., Livingston, G., and Groot, W. d.: Effects of fires on carbon cycling in North American boreal peatlands, Environmental Reviews, 6, 13–24, https://doi.org/10.1139/a98-002, 1998.
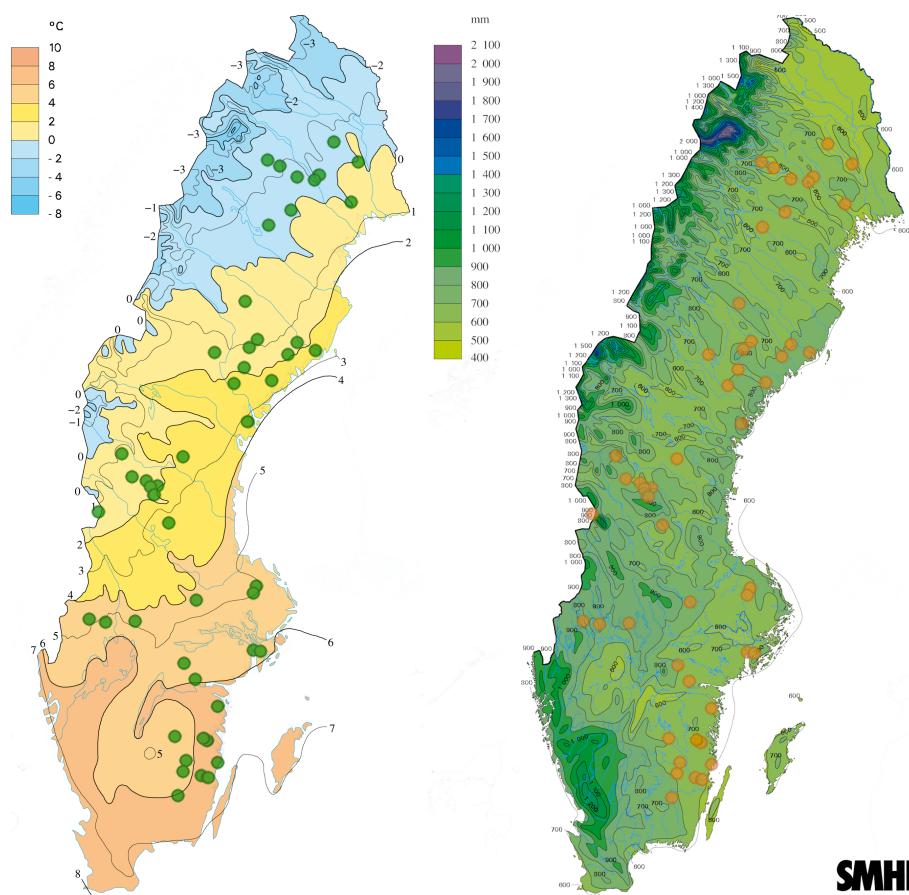
Figure 1. Using climate data averaged over the period 1961-2017 provided by the Swedish Meteorological and Hydrological Institute (SMHI) for plot selection, MAT had a range of 0.43-7.77 °C and MAP of 539-772 mm over an approximately 57-67° latitudinal change. The 50 plot pairs are pictured as points upon MAT and MAP gradients over the last normal period 1961-1990.
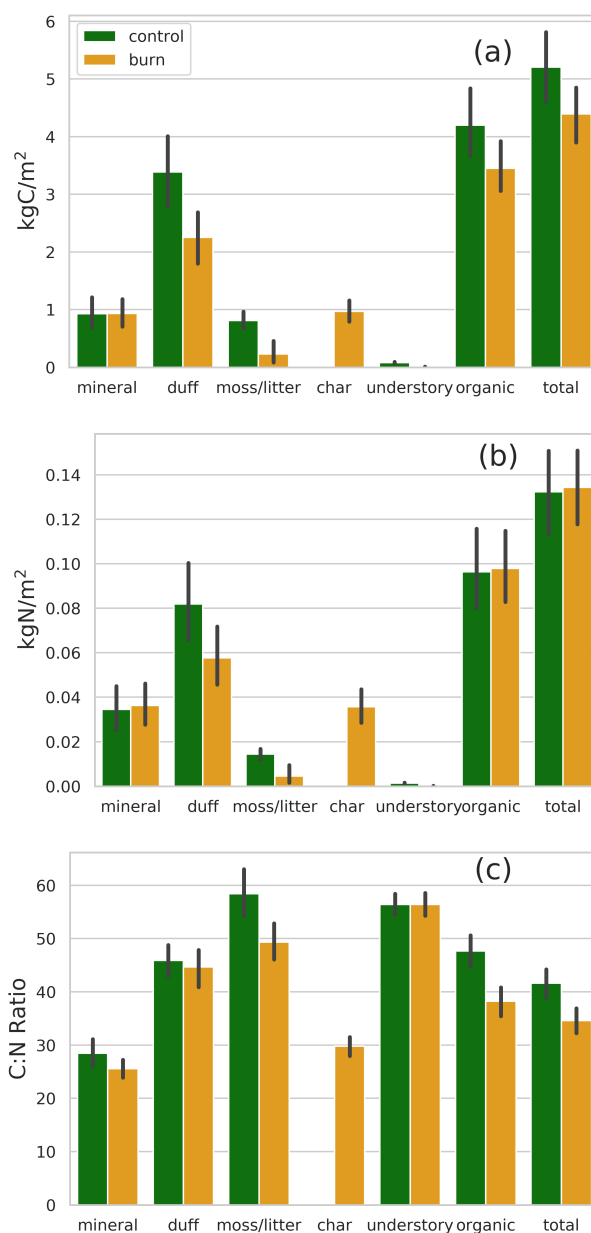
Figure 2. Mean C (a) and N (b) stocks and their ratio (c) between burn and control plots amongst forest compartments. Error bars are the bootstrapped 95% confidence interval of the mean.
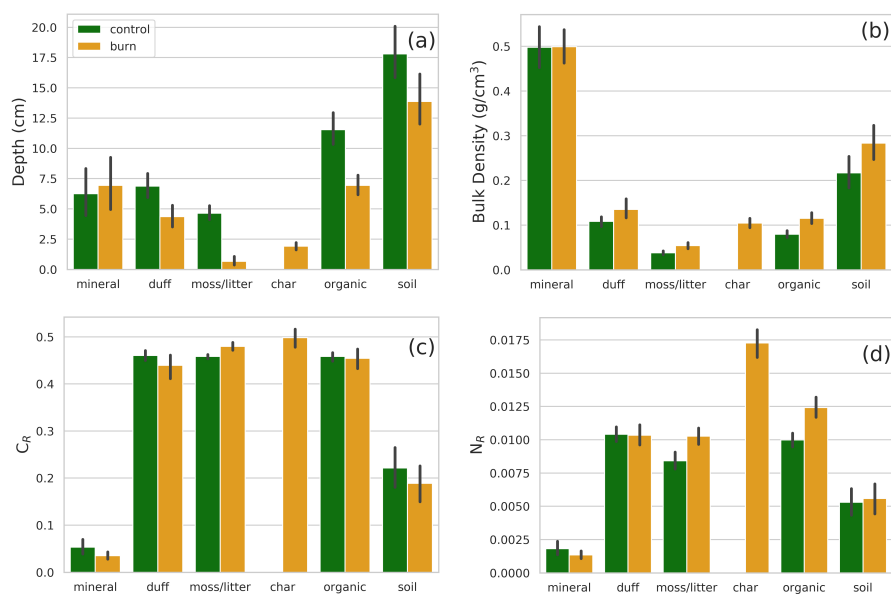
Figure 3. Mean soil compartment depths (a), bulk density (b), C_R (c), and N_R (d) in burn and control plots. Error bars are the bootstrapped 95% confidence interval of the mean.
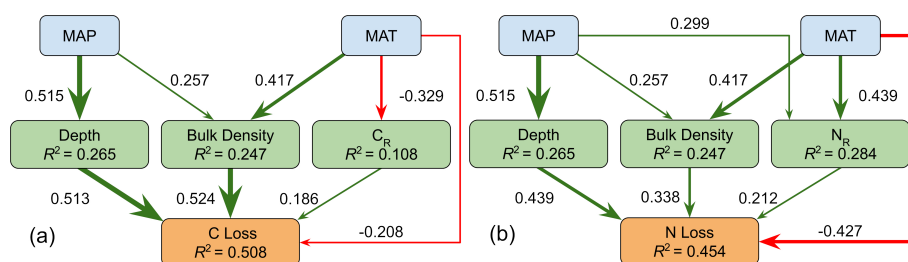
Figure 4. Diagram of proposed pathways for the effects of MAP and MAT on C (a) and N (b) loss. Non climate variables regard the organic layer. Each variable node is labeled with the R^2 from simple or multiple regression using explanatory variables represented by all incoming arrows. Arrows are labeled by and sized in proportion to the magnitude of their standardized regression coefficients. Green arrows represent positive relationships while red represent negative relationships.
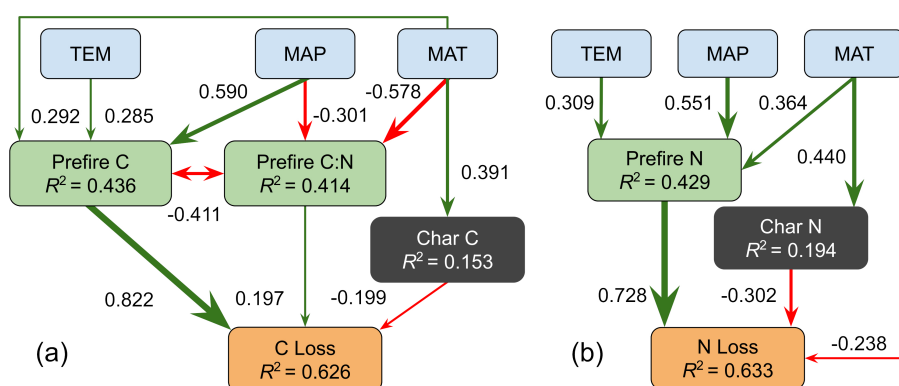
Figure 5. Path diagrams for C (a) and N (b) loss including char and C:N variables. Prefire C, N, and C:N as well as losses of C and N are regarding the organic layer. Each variable node is labeled with the R^2 from simple or multiple regression using explanatory variables represented by all incoming arrows. Arrows are labeled by and sized in proportion to the magnitude of their standardized regression coefficients. Green arrows represent positive relationships while red represent negative relationships.

Table 1. Mean values of distributions ($n = 50$) formed by subtracting control plot variables from their paired burn plot. In parentheses are first the 95% confidence interval of the distribution and then the percentage change calculated from the overall means of control and burn plots. Statistically significant fire induced changes are in bold.

	C (kg/m^2)	N (kg/m^2)	C:N
Total	**-0.815 (0.652, -15.6)**	0.00208 (0.0184, 1.6)	**-7.01 (2.58, -16.8)**
Understory	**-0.0717 (0.0126, -90.6)**	**-0.00127 (0.000224, -90.6)**	– (–, –)
Soil	**-0.744 (0.651, -14.5)**	0.00336 (0.0184, 2.6)	**-6.88 (2.61, -16.6)**
Organic	**-0.747 (0.633, -17.8)**	0.00157 (0.0187, 1.6)	**-9.46 (2.97, -19.8)**
Char	**0.971 (0.182, –)**	**0.0357 (0.00799, –)**	– (–, –)
Moss/Litter	**-0.584 (0.258, -72.0)**	**-0.00985 (0.00490, -68.2)**	**-9.09 (4.01, -15.6)**
Duff	**-1.13 (0.581, -33.5)**	**-0.0242 (0.0173, -29.6)**	-1.24 (3.32, -2.7)
Mineral	0.00333 (0.248, 0.4)	0.00179 (0.00834, 5.2)	**-3.11 (2.46, -10.2)**

Table 2. Mean values of distributions ($n = 50$) formed by subtracting control plot variables from their paired burn plot. In parentheses are first the 95% confidence interval of the distribution and then the percentage change calculated from the overall means of control and burn plots. Statistically significant fire induced changes are in bold.

	Depth (cm)	Bulk Density (g/cm^3)	C_r	N_r
Soil	**-3.92 (1.47, -22.0)**	**0.0665 (0.0305, 30.7)**	-0.0326 (0.0395, -14.7)	0.000286 (0.00104, 5.4)
Organic	**-4.60 (1.19, -39.9)**	**0.0358 (0.0110, 45.0)**	-0.00402 (0.0193, -0.9)	**0.00243 (0.000801, 24.3)**
Char	**1.91 (0.292, –)**	– (–, –)	– (–, –)	– (–, –)
Moss/Litter	**-3.98 (0.762, -85.6)**	**0.0162 (0.00568, 42.8)**	**0.0215 (0.00828, 4.7)**	**0.00185 (0.000727, 21.9)**
Duff	**-2.53 (1.04, -36.8)**	**0.0270 (0.0190, 24.9)**	-0.0212 (0.0239, -4.6)	-0.0000714 (0.000714, -0.7)
Mineral	0.684 (1.32, 10.9)	0.00565 (0.0352, 0.283)	**-0.0199 (0.0127, -34.2)**	**-0.000505 (0.000369, -25.8)**